An investigation of the $KL_{2,3}$ to $L_{2,3}L_{2,3}$ V Auger satellites of Mg and Al

1990 J. Phys.: Condens. Matter 2 9949

(http://iopscience.iop.org/0953-8984/2/49/019)

J. Phys.: Condens. Matter 2 (1990) 9949–9959. Printed in the UK

An investigation of the $KL_{2,3} \rightarrow L_{2,3}L_{2,3}$ V Auger satellites of Mg and Al

A D Laine†, P S Fowles†, G Cubiotti‡, J E Inglesfield§, S D Waddington‖ and P Weightman†

† Department of Physics and Surface Science Research Centre, University of Liverpool, Liverpool L69 3BX, UK

‡ Istituto di Fisica Teorica, Università, Messina, 98100 Italy

§ Institute of Theoretical Physics, Catholic University of Nijmegen, Toernooiveld, Nijmegen, The Netherlands

‖ ICI P&P Division, Wilton, Middlesbrough, Cleveland T36 8JE, UK

Received 2 July 1990, in final form 10 September 1990

Abstract. The $KL_{2,3} \rightarrow L_{2,3}L_{2,3}$ V Auger vacancy satellite transitions of Mg and Al, which lie to high kinetic energy of the $KL_{2,3}$ V Auger profile, are analysed using a combination of self-consistent densities of states (DOS) and atomic-like Auger transition rate calculations. The transition rate calculations demonstrate that previous work based on statistical weight arguments is incorrect. The DOS calculations show that the valence s contribution to the local DOS forms a bound state in the presence of a double core-hole state, though the major contribution to the core-hole screening is provided by the local p DOS. The calculation successfully reproduces the spectral profile for the Al transitions, but is unable to account for one of the features in the Mg spectrum.

1. Introduction

Considerable attention has been focused on understanding the Auger spectra of simple metals such as Mg and Al [1–8], and the main features of the transitions that create single and double valence holes in the final state are now well understood [5–8]. The study of CVV and CCV transitions in simple metals can give insight into the mechanisms of screening single core-hole states.

It is also possible for the exciting x-rays to generate doubly ionized shake-up states, and recent observations of Auger vacancy satellite processes arising from the decay of such states opens up the possibility of studying the screening of doubly ionized core-hole states. One such process is the $KL_{2,3} \rightarrow L_{2,3}L_{2,3}$ V transition, which is observed as a satellite spectrum to high kinetic energy of the $KL_{2,3}$ V profile, and it is to this that we address ourselves in this paper.

It is difficult to perform calculations relating to Auger transitions of the $KL \rightarrow L^2V$ type owing to the complexity of the multiplet structure arising from the angular momentum coupling of the core holes. Previously, these transitions have been measured in Al and Mg, and attempts have been made to simulate the lineshape by associating the experimental $KL_{2,3}V$ profile with each transition between the $KL_{2,3}$ initial states and the $L_{2,3}L_{2,3}$ V final states [9, 10]. The final-state intensities and the relative populations of

0953-8984/90/499949 + 11 $03.50

the initial-state multiplets were used as free parameters in order to obtain a fit to the data. This procedure was found to give a reasonable fit to the data for the case of Mg, but several structures were found in the $KL_{2,3} \rightarrow L_{2,3}L_{2,3}$ V spectrum of Al that could not be explained in this way.

In this work, we make a further attempt to account for the profile of these satellite transitions and to gain an insight into the screening around a doubly ionized site. According to the final-state rule [11–16], the intensities of the components of an Auger spectrum are determined by the initial state and the shapes by the final state. Consequently, the intensities of the multiplet components of the initial state have been computed using atomic-like Auger transition rate calculations and the lineshapes represented firstly by the s and p partial local densities of states (DOS) and secondly by the s and p components of the $KL_{2,3}$ V profile, both calculated in the presence of two final-state core holes. The relative positions of each of the different features in the spectra were found from Hartree–Fock calculations.

2. Experiment

The $KL_{2,3} \rightarrow L_{2,3}L_{2,3}$ V Auger spectrum of Mg has been previously determined by Davies *et al* [9] using a modified AEI ES200 electron spectrometer [17]. The specimen was prepared by cathodic sputtering of Mg onto an Al substrate in the presence of an argon atmosphere of 3×10^{-2} Torr. This spectrum has subsequently been reproduced with a solid polycrystalline sample cleaned by creating a new surface via mechanical scraping.

The Al $KL_{2,3} \rightarrow L_{2,3}L_{2,3}$ V spectrum has also been measured previously [10]. In this case Al was sputtered onto a Cu substrate and Si x-rays used as the excitation source. It is believed that the shape of this spectrum was influenced to some degree by the presence of the Cu substrate, possibly by the diffusion of Cu into the Al layer. The spectrum has thus been remeasured from a solid specimen of 99.9% pure Al, with the sample being scraped every 2.5 h. The remeasured data were obtained using Ti x-rays with a data collection time of 50 h, during which the oxygen and carbon contamination levels were found to be <0.1 and <0.2 monolayers respectively, as determined from photoelectron cross sections [18] and escape depths [19].

3. Theory

The analysis of complex Auger spectra requires a knowledge of the relative position, intensity and shape of each of the spectral components present. For Mg, the initial- and final-state splittings were extracted from the Hartree–Fock calculations of Breuckmann and Schmidt [20], whilst the configurational average was obtained from the difference of two self-consistent field Hartree–Fock (ΔSCF) calculations within the excited atom model as described by Jennison *et al* [21]. For Al, the position of each component was also calculated within the ΔSCF scheme. There remains some uncertainty in the configurational average, due in part to the neglect of relativity, which is of the order of several eV for the K shells of Mg and Al. The theoretical values obtained for the position

Table 1. The energies of Auger transitions in Mg.

	KE^F (eV)		
Transition	Theory	Experiment	Δ†
$K \rightarrow L_1V$	1211.4	1214.4 (2)	3.0
$K \rightarrow L_{2,3}V$	1250.5	1253.3 (2)	2.8
$KL_{2,3}(^1P) \rightarrow L_{2,3}L_{2,3}(^1S)V$	1254.6	—	
$KL_{2,3}(^1P) \rightarrow L_{2,3}L_{2,3}(^1D)V$	1259.0	—	
$KL_{2,3}(^1P) \rightarrow L_{2,3}L_{2,3}(^3P)V$‡	1263.5	—	
$KL_{2,3}(^3P) \rightarrow L_{2,3}L_{2,3}(^1S)V$‡	1248.6	—	
$KL_{2,3}(^3P) \rightarrow L_{2,3}L_{2,3}(^1D)V$‡	1253.0	—	
$KL_{2,3}(^3P) \rightarrow L_{2,3}L_{2,3}(^3P)V$	1257.5	—	

† Δ = experiment − theory.
‡ Indicates that this transition is found not to occur.

Table 2. The energies of Auger transitions in Al.

	KE^F (eV)		
Transition	Theory	Experiment	Δ†
$K \rightarrow L_1V$	1437.9	1441.6 (1)	3.7
$K \rightarrow L_{2,3}V$	1482.4	1486.7 (1)	4.3
$KL_{2,3}(^1P) \rightarrow L_{2,3}L_{2,3}(^1S)V$	1485.7	—	
$KL_{2,3}(^1P) \rightarrow L_{2,3}L_{2,3}(^1D)V$	1493.4	—	
$KL_{2,3}(^1P) \rightarrow L_{2,3}L_{2,3}(^3P)V$‡	1498.5	—	
$KL_{2,3}(^3P) \rightarrow L_{2,3}L_{2,3}(^1S)V$‡	1479.1	—	
$KL_{2,3}(^3P) \rightarrow L_{2,3}L_{2,3}(^1D)V$‡	1486.7	—	
$KL_{2,3}(^3P) \rightarrow L_{2,3}L_{2,3}(^3P)V$	1491.8	—	

† Δ = experiment − theory.
‡ Indicates that this transition is found not to occur.

of each component may be seen in table 1 for Mg and table 2 for Al. Also shown are the predicted and experimental values for the positions of the KL_1 V and $KL_{2,3}$ V Auger transitions. The theory underestimates experiment by about 3–4 eV, and it is expected that this will also be the case for the satellite transitions.

3.1. The Auger transition rate calculations

The intensities of each of the components of the Auger spectrum were obtained from the atomic-like transition rate calculations of Laine *et al* [22–25], which use the formalism of McGuire [26]. In this technique the initial state is described in the *jj* coupling scheme and the final state in the *LS* coupling scheme. The transition rate may then be calculated providing the matrix element linking the initial and final states is known. For many free atoms these have already been tabulated by McGuire [27, 28] using wavefunctions obtained from Hermann and Skillman's atomic structure calculations [29]. These calculations relate to an isolated atom and their applicability to the solid state has been

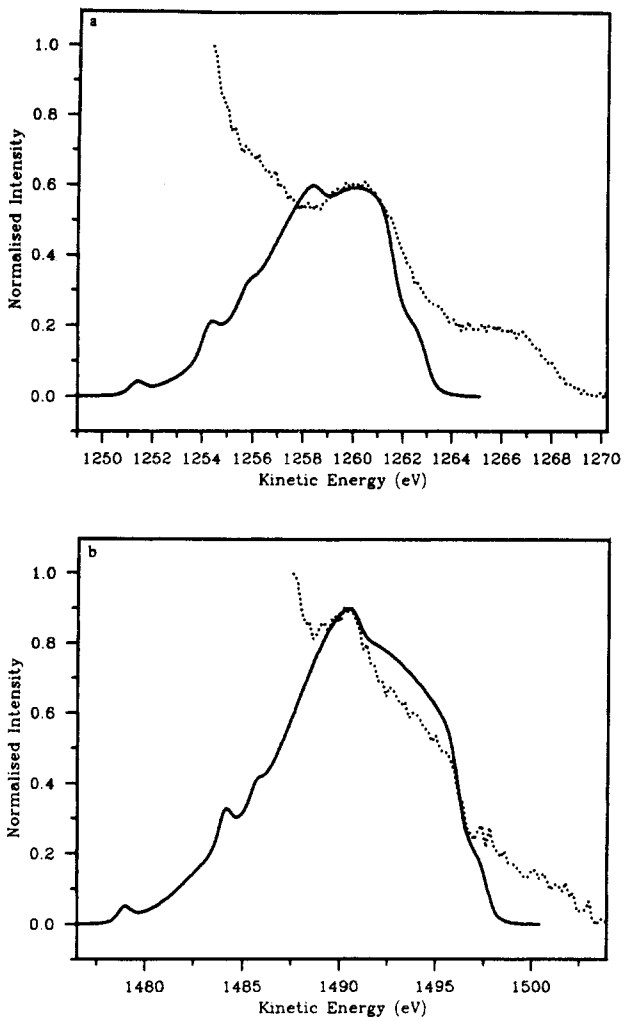

Figure 1. A comparison of experimental and theoretical profiles for the $KL_{2,3} \rightarrow L_{2,3}L_{2,3}\,V$ Auger transition in (*a*) Mg and (*b*) Al. The theory is shown by the full curve and the experiment by the dotted curve.

discussed elsewhere [22, 30]. In this procedure the valence configuration that surrounds the two core-hole initial state may be chosen in order to simulate the valence screening. Different populations of the 3s and 3p initial valence states give rise to different $KL_{2,3} \rightarrow L_{2,3}L_{2,3}\,V_s$: $KL_{2,3} \rightarrow L_{2,3}L_{2,3}\,V_p$ intensity ratios, where V_s and V_p indicate that the emitted Auger electron comes from an s or p valence state respectively.

3.2. The lineshapes of the Auger satellite components

Each component of the Auger satellite structure has an associated lineshape, which reflects the two core-hole local DOS. In order to simulate this, the embedding technique [8, 31] was applied to an atom with two core holes embedded in a free-electron host. The lineshape was then found in two ways by obtaining the s and p contributions to (i)

Table 3. Satellite transition rates for magnesium.

Initial valence configuration	$KL_{2,3} \rightarrow L_{2,3}L_{2,3}V_s$ Transition rate ($\times 10^{-4}$ au)			
	$^1P \rightarrow {}^1S$	$^1P \rightarrow {}^1D$	$^3P \rightarrow {}^3P$	Total
$3s^13p^1$	0.06	0.31	0.56	0.94
$3s^13p^3$	0.19	0.94	1.69	2.81
$3s^23p^0$	0.13	0.63	1.13	1.88
$3s^23p^1$	0.13	0.63	1.13	1.88
$3s^23p^2$	0.38	1.88	3.38	5.63
$3s^23p^3$	0.38	1.88	3.38	5.63

Initial valence configuration	$KL_{2,3} \rightarrow L_{2,3}L_{2,3}V_p$ Transition rate ($\times 10^{-4}$ au)			
	$^1P \rightarrow {}^1S$	$^1P \rightarrow {}^1D$	$^3P \rightarrow {}^3P$	Total
$3s^13p^1$	0.09	0.43	0.78	1.30
$3s^13p^3$	1.37	6.86	12.34	20.57
$3s^23p^0$	0.00	0.00	0.00	0.00
$3s^23p^1$	0.09	0.43	0.78	1.30
$3s^23p^2$	0.52	2.59	4.67	7.78
$3s^23p^3$	1.37	6.86	12.34	20.57

the $KL_{2,3}$ V Auger transition in the presence of a 2p spectator hole and (ii) the local DOS influenced by two 2p core holes. The calculation of both the $KL_{2,3}$ V profile and the local DOS allows the effect of the energy dependence of the matrix elements, which proved to be important for the KL_1 V transition, to be assessed [8]. The amount of screening charge was determined by integrating the density of states up to the Fermi energy and the Wigner–Seitz radius.

Once the shapes of the valence s and p contributions to the lineshape have been determined, it is necessary to weight these using the transition rate calculations. This is done by equating the area of the s and p contributions obtained to the total transition rates, $KL_{2,3} \rightarrow L_{2,3}L_{2,3}V_s$ and $KL_{2,3} \rightarrow L_{2,3}L_{2,3}V_p$ respectively, for each satellite component.

4. Results

4.1. Experimental results

The Mg $KL_{2,3} \rightarrow L_{2,3}L_{2,3}$ V spectrum is shown by the dots in figure 1(*a*). It lies to high kinetic energy of the $KL_{2,3}$ V Auger transition, which affects the low-kinetic-energy region of the spectrum, but is very much weaker in intensity. There are two broad peaks, the first centred at ~1260 eV and the second at ~1266 eV. The region to higher kinetic energy shows a flat, featureless background.

The Al $KL_{2,3} \rightarrow L_{2,3}L_{2,3}$ V spectrum, shown by the dots in figure 1(*b*), is markedly different in shape from that of Mg. The spectrum consists of a peak at 1491 eV and a

Table 4. Satellite transition rates for aluminium.

Initial valence configuration	$KL_{2,3} \rightarrow L_{2,3}L_{2,3}V_s$ Transition rate ($\times 10^{-4}$ au)			
	$^1P \rightarrow {}^1S$	$^1P \rightarrow {}^1D$	$^3P \rightarrow {}^3P$	Total
$3s^13p^2$	0.22	1.08	1.95	3.25
$3s^13p^3$	0.22	1.08	1.95	3.25
$3s^13p^4$	0.22	1.08	1.95	3.25
$3s^23p^1$	0.15	0.72	1.30	2.17
$3s^23p^2$	0.44	2.17	3.90	6.51
$3s^23p^3$	0.44	2.17	3.90	6.51

Initial valence configuration	$KL_{2,3} \rightarrow L_{2,3}L_{2,3}V_p$ Transition rate ($\times 10^{-4}$ au)			
	$^1P \rightarrow {}^1S$	$^1P \rightarrow {}^1D$	$^3P \rightarrow {}^3P$	Total
$3s^13p^2$	0.52	2.59	4.67	7.78
$3s^13p^3$	1.37	6.86	12.34	20.57
$3s^13p^4$	2.96	14.80	26.64	44.40
$3s^23p^1$	0.09	0.43	0.78	1.30
$3s^23p^2$	0.52	2.59	4.67	7.78
$3s^23p^3$	1.37	6.86	12.34	20.57

broad feature from 1492 to 1496 eV. To higher kinetic energy there is a background with no sharp features.

4.2. Transition rates

The initial-state 1s and 2p core holes for the $KL_{2,3} \rightarrow L_{2,3}L_{2,3}$ V transition give rise to ^1P and ^3P initial states. Similarly, the two final-state 2p core holes mix to give ^1S, ^3P and ^1D final states. Any splitting due to the valence configuration interaction is negligible. The problem is simplified somewhat since transitions from a singlet initial state to a triplet final state and from a triplet initial state to a singlet final state are found to be forbidden. For the transitions that do exist, the transition rate varies as the statistical weight of the final states, i.e. the ratio of $^1S : {}^1D : {}^3P$ is found to be 1:5:9. Tables 3 and 4 show the transition rates calculated for various screening configurations in Mg and Al.

Table 5 shows the configuration, found from the embedding calculation, for the s and p valence electrons for Al and Mg in the presence of zero, one and two core holes. Interest is focused in this case on the configuration due to two core holes, and it may be noted that the values obtained for the numbers of s and p electrons are non-integer. Unfortunately, the nature of the atomic rate calculations of Laine *et al* is such that only integer numbers of electrons are permitted, and as such it is necessary to interpolate between these values to obtain a value of $KL_{2,3} \rightarrow L_{2,3}L_{2,3}\,V_s : KL_{2,3} \rightarrow L_{2,3}L_{2,3}\,V_p$ for the required number of s and p electrons, as discussed in section 4.4.

4.3. Two core-hole Auger profiles and local densities of states

The calculated local DOS and the s and p components of the $KL_{2,3}$ V profile, in the presence of two core holes, for Mg are shown in figure 2. Similar results are obtained

Table 5. The valence screening charge for aluminium and magnesium.

	Valence screening charge (e^-)			
	Mg		Al	
No of core holes (ΔZ)	3s	3p	3s	39
$\Delta Z = 0$	1.0	1.0	1.2	1.9
$\Delta Z = 1$	1.4	1.6	1.6	2.6
$\Delta Z = 2$	1.5	2.5	1.7	3.5

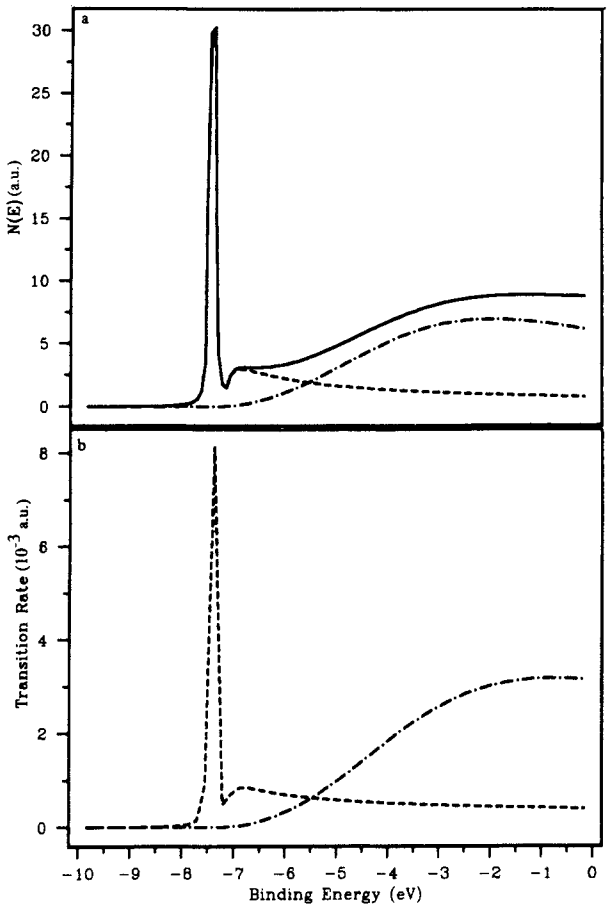

Figure 2. The calculated profiles of Mg for (*a*) the two core-hole local DOS and (*b*) the s and p components of the $KL_{2,3}V$ Auger transition in the presence of a 2p spectator core hole. The full curve represents the total, and the s and p contributions are represented by broken and chain curves respectively.

for Al. In both cases the p local DOS is little changed in shape from that of the singly ionized and neutral atom, the most notable change being the movement of the maximum value from the Fermi edge towards the centre of the valence band. By comparison the s local DOS shows great modification from the singly ionized and neutral atom. The attractive potential created by the two core holes is sufficient to create an s-like bound state, which is pulled just below the bottom of the valence band, in addition to distorting the shape of the band itself.

The s and p contributions to the $KL_{2,3}V$ profiles of both Mg and Al reflect closely the shapes of the equivalent parts of the local DOS. The most noticeable divergence in shape between the local DOS and the Auger profile is the position of the maximum value of the p contribution, which lies closer to the Fermi edge in the Auger profile than the density of states. Clearly in this instance, unlike the situation for the KL_1V of Mg [8], the energy dependence of the matrix elements does not play a significant role in determining the shape of the s and p components to be used for this work.

4.4. Satellite profiles for Al and Mg

In this attempt to simulate the satellite spectrum the lineshapes obtained in section 4.3 were used as a starting point. The transition rate calculations in tables 3 and 4 were used to find the lineshape of each component of the satellite transition as described in section 3.2. These individual components were then summed, having first been split by the energies obtained from the results of the Hartree–Fock calculations. The spectra were then broadened by a Lorentzian to simulate lifetime effects of the K and $L_{2,3}$ core levels (0.38 eV for Mg and 0.45 eV for Al) and by a Gaussian of 0.5 eV to simulate the instrumental resolution. The embedding calculations carried out indicated that valence configurations of $3s^{1.5}3p^{2.5}$ and $3s^{1.7}3p^{3.5}$ are appropriate for the screening of Mg and Al respectively. Since it was not possible to calculate the transition rate for a fractional number of electrons, the required transition rate was obtained using a linear interpolation between, for Mg, $3s^13p^3$ and $3s^23p^2$, and, for Al, $3s^13p^4$ and $3s^23p^3$, since these screening configurations contain the appropriate number of screening electrons to ensure charge neutrality. Figure 3 shows the three profiles obtained for Mg with four valence screening electrons: the profiles corresponding to the two integer charge configurations and the interpolated value derived from the embedding procedure. These show three small peaks at low binding energy due to the s contributions along with three distinct edges due to the p contributions. Similar results are obtained for Al.

5. Discussion

Previous analysis [9, 10] of the satellite spectra of both Mg and Al have assumed that each initial state (^1P and ^3P) could decay to all available final states (^3P, ^1S and ^1D). The transition rate calculations show that this procedure was erroneous since several of the transitions are forbidden.

The calculated densities of states are striking because of the creation of a bound state which is pulled from the bottom of the band. The strong distortion of the s local DOS is not so surprising in the light of results [8] which show that the double-peaked structure of Mg and Al KL_1V Auger transitions may be attributed to the change in the shape of the s contribution as compared to the ground-state DOS [4]. More surprising, perhaps, is the orbital character of the screening by the valence electrons; this study shows that the screening is predominantly p-like in character, as shown in table 5. This result is at

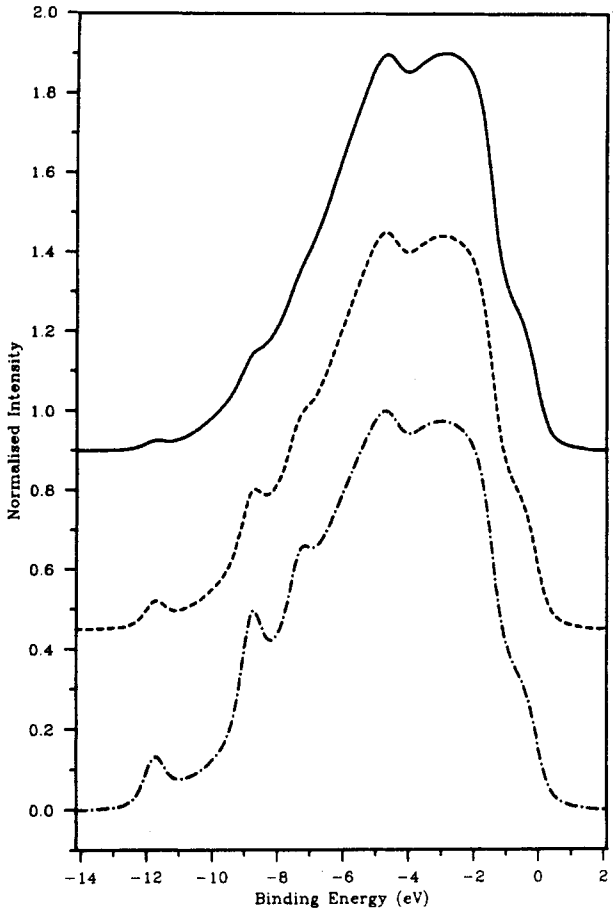

Figure 3. The theoretically generated $KL_{2,3} \rightarrow L_{2,3}L_{2,3}$ V Auger profiles for Mg. The full, broken and chain curves represent the valence screening configurations of $3s^{1}3p^{3}$, $3s^{1.5}3p^{2.5}$ and $3s^{2}3p^{2}$, respectively.

variance with some earlier studies of core-hole screening in simple metals [5, 21] but is in agreement with more recent work [6–8, 22], which shows that although the *shape* of the local s DOS is strongly distorted the *shape* of the local p DOS is largely unaffected. However, the *magnitude* of the s charge is little changed whereas that of the p charge is greatly increased. It is for this reason that the screening is described as p-like when the more obvious changes lie in the s local DOS.

The simulated satellite spectra show three small peaks to low kinetic energy. These are followed by three broad features: for Mg, the first two of these (due to the ^{1}S and ^{3}P) almost merge; for Al, these peaks are more readily resolved due to the different ^{1}S and ^{3}P final-state splittings.

The calculated lineshapes may now be compared with the experimentally determined spectra. The three narrow features, which appear in the lower energy region of the calculated profile, are located under the tail of the $KL_{2,3}$ V Auger transition and hence will not be observable. It is unlikely in any case that these could be resolved, since, as was noted in the case of the Mg $KL_{2,3}$ V transition [8], the Auger profile seems to be

broader than the contributions of the K and $L_{2,3}$ core levels alone would suggest. This is probably due to lifetime effects in the valence band, the broadening increasing towards the bottom of the band, and so any such small features in the experimental spectra are likely to be obscured. The theoretical values obtained for the positions of the Fermi energy of the Auger transitions underestimate the values by several eV. In order to fit the Auger satellite spectra of Mg and Al, energy shifts of 4.0 eV and 5.0 eV respectively have been added to the energy scale of the calculated spectra. As can be seen from tables 1 and 2 this is consistent with the energy shift necessary to align the experimental and theoretical Fermi energies of the KL_1 V and $KL_{2,3}$ V transitions.

For Mg (figure 1(*a*)), the most intense feature in the experimental spectrum is matched closely in energy by the two almost merged calculated peaks, and is thus attributed to transitions to the ^1S and ^3P final states. To higher energy there is a gently sloping region corresponding to the Fermi energy of the transition to the ^1D final state. This leaves one remaining feature at 1266 eV that is not accounted for by these calculations. Its position corresponds to no direct or internal photoemission line, nor to any plasmon loss or gain satellite. Since the unidentified feature appears at an energy corresponding to that of the forbidden $^1P \rightarrow {}^3P$ transition, it is possible (though we feel unlikely) that the feature is due to a breakdown of the *LS* coupling scheme used to calculate the transition rates. It is likely that, given its width, this unidentified feature arises from a transition involving a valence electron. It may be that it is a $KL_{2,3}$ V Auger satellite process taking place in the presence of two spectator holes.

The agreement between experiment and theory for Al is much more satisfactory (figure 1(*b*)) due to the absence of unexplained peaks. The feature at 1491 eV may clearly be associated with the Fermi energy of the ^1S final state, while the region from 1492 to 1496 eV is due to the ^3P final state. The Fermi edge of the high-energy part of the spectrum is indistinct but may be assigned to the ^1D final state. The spectrum may hence be explained within the limitations of the unknown background present.

6. Conclusions

The $KL_{2,3} \rightarrow L_{2,3}L_{2,3}$ V Auger satellite spectra of Mg and Al have been modelled using a combination of atomic transition rates and self-consistently calculated lineshapes in the presence of two core holes. The final state of the system has two core holes in the 2p level and transitions to the three terms of this configuration vary with statistical weight, i.e. the intensity ratio of the $^1S:{}^1D:{}^3P$ is 1:5:9. The ratio between the $KL_{2,3} \rightarrow L_{2,3}L_{2,3}\,V_s$ and $KL_{2,3} \rightarrow L_{2,3}L_{2,3}\,V_p$ rates is found to vary greatly as a function of the screening charge. In order to try and find the correct transition rate for the non-integer valence charge, it was necessary to interpolate between these values. Since the features due to the $KL_{2,3} \rightarrow L_{2,3}L_{2,3}\,V_s$ transitions are obscured by the high-energy tail of the $KL_{2,3}$ V spectrum, it has not been possible to determine the success of this procedure.

The calculated local DOS have shown the formation of an s-like bound state just below the band and a p contribution largely unchanged in shape but which provides the majority of the valence screening.

The approach used in this work simulates well the satellite structure of Al, but for Mg leaves one of the observed features unexplained. This may be due to a further satellite transition that occurs in the presence of two spectator core holes.

In order for further progress to be made it is necessary to obtain spectra in which the satellite transition will be enhanced, possibly by means of electron or proton excitation

in which a greater number of two core-hole initial states are created than in x-ray excitation.

References

[1] Jackson A J, Tate C, Gallon T E, Basset P J and Matthew J A D 1975 *J. Phys. F: Met. Phys.* **5** 363
[2] Fuggle J 1977 *J. Phys. F: Met. Phys.* **7** L81
[3] Barò A M and Tagle J A 1978 *J. Phys. F: Met. Phys.* **8** 563
[4] Lässer R and Fuggle J C 1980 *Phys. Rev.* B **22** 2637
[5] Davies M, Jennison D R and Weightman P 1984 *Phys. Rev.* B **29** 5313
[6] Almbladh C O, Morales A L and Grossmann G 1989 *Phys. Rev.* B **39** 3489
[7] Almbladh C O and Morales A L 1989 *Phys. Rev.* B **39** 3503
[8] Fowles P S, Inglesfield J E and Weightman P 1990 to be published
[9] Davies M, Jennison D R and Weightman P 1984 *J. Phys. C: Solid State Phys.* **17** L107
[10] Hannah P H and Weightman P 1985 *J. Phys. C: Solid State Phys.* **18** L239
[11] Jennison D R 1978 *Phys. Rev. Lett.* **40** 807
[12] Jennison D R, Madden H H and Zehner D M 1980 *Phys. Rev.* B **21** 430
[13] von Barth U and Grossmann G 1980 *Phys. Scr.* **21** 580
[14] von Barth U and Grossmann G 1982 *Phys. Rev.* B **25** 5150
[15] von Barth U and Grossmann G 1983 *Phys. Scr.* **28** 107
[16] Ramaker D E 1982 *Phys. Rev.* B **25** 7341
[17] Weightman P and Andrews P T 1980 *J. Phys. C: Solid State Phys.* **13** 3529
[18] Scofield J H 1976 *J. Electron. Spectrosc.* **9** 29
[19] Penn D R 1976 *J. Electron. Spectrosc.* **8** 129
[20] Breuckmann B and Schmidt V 1974 *Z. Phys.* **268** 235
[21] Jennison D R, Weightman P, Hannah P H and Davies M 1984 *J. Phys. C: Solid State Phys.* **17** 3701
[22] Laine A D, Cubiotti G and Weightman P 1990 *J. Phys.: Condens. Matter* **2** 2421
[23] Cubiotti G, Laine A D and Weightman P 1989 *J. Phys.: Condens. Matter* **1** 7723
[24] Laine A D, Cubiotti G and Weightman P 1989 *J. Phys.: Condens. Matter* **1** SB263
[25] Laine A D, Cubiotti G and Weightman P 1989 *Auger Spectroscopy and Electronic Structure* (Berlin: Springer)
[26] McGuire E J 1975 *Atomic Inner Shell Processes* (New York: Academic)
[27] McGuire E J 1969 *Phys. Rev.* **185** 1
[28] McGuire E J 1970 *Phys. Rev.* A **2** 273
[29] Hermann F and Skillman S 1963 *Atomic Structure Calculations* (Englewood Cliffs, NJ: Prentice-Hall)
[30] Weightman P 1982 *Rep. Prog. Phys.* **45** 753
[31] Inglesfield J E 1981 *J. Phys. C: Solid State Phys.* **14** 3795